Transcriptome Analysis of *Drosophila melanogaster* Third Instar Larval Ring Glands Points to Novel Functions and Uncovers a Cytochrome p450 Required for Development

Danielle Christesen, Ying Ting Yang, Jason Somers,[1] Charles Robin, Tamar Sztal,[2] Philip Batterham, and Trent Perry[3]

School of Biosciences, Bio21 Molecular Science and Biotechnology Institute, The University of Melbourne, Parkville, Victoria 3010, Australia

ABSTRACT In *Drosophila melanogaster* larvae, the ring gland (RG) is a control center that orchestrates major developmental transitions. It is a composite organ, consisting of the prothoracic gland, the corpus allatum, and the corpora cardiaca, each of which synthesizes and secretes a different hormone. Until now, the RG's broader developmental roles beyond endocrine secretion have not been explored. RNA sequencing and analysis of a new transcriptome resource from *D. melanogaster* wandering third instar larval RGs has provided a fascinating insight into the diversity of developmental signaling in this organ. We have found strong enrichment of expression of two gene pathways not previously associated with the RG: immune response and fatty acid metabolism. We have also uncovered strong expression for many uncharacterized genes. Additionally, RNA interference against RG-enriched cytochrome p450s *Cyp6u1* and *Cyp6g2* produced a lethal ecdysone deficiency and a juvenile hormone deficiency, respectively, flagging a critical role for these genes in hormone synthesis. This transcriptome provides a valuable new resource for investigation of roles played by the RG in governing insect development.

Endocrine control of insect development is a complex symphony, with hormones produced in overlapping waves that determine the timing and nature of each developmental transition. In *Drosophila melanogaster* larvae, an endocrine organ, the ring gland (RG), is the control center that produces many of these hormones to orchestrate larval molts and the larval-pupal transition.

Located anterior to the larval central nervous system (CNS), the RG is a composite organ consisting of three different subtissues (King *et al.* 1966) (see Figure 1), each of which synthesizes and secretes a different hormone. The prothoracic gland (PG) is the major subtissue of the RG, both by size and cell number (King *et al.* 1966). The PG synthesizes the insect molting hormone ecdysone (Vogt 1943; Wigglesworth 1954), which is released into the hemolymph for conversion to its active form 20-hydroxyecdysone (20E) at peripheral target tissues (Petryk *et al.* 2003). 20E directly triggers major developmental events in the larva, and its precursor ecdysone is secreted by the PG cells in clearly defined pulses to provide temporal control of these events; there is a single pulse prior to each larval molt, prior to pupariation, and at the commencement of metamorphosis (Riddiford 1993; reviewed in Baehrecke 1996; Thummel 2002; Ou and King-Jones 2013).

The second-largest RG subtissue is the corpus allatum (CA) (King *et al.* 1966). Throughout the first and second larval instars, the CA cells synthesize and secrete juvenile hormone (JH), which determines the nature of all 20E-induced transitions (Williams 1961; Bownes and Rembold 1987; Sliter *et al.* 1987). In the presence of JH, 20E will always trigger a larval-larval molt (Riddiford 1970). Upon attainment of critical weight early in the third larval instar, JH production at the CA ceases, allowing
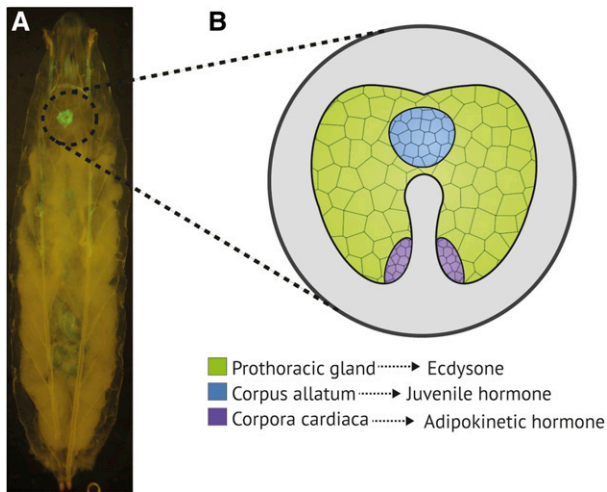
Figure 1 Position and substructure of the *D. melanogaster* third instar larval RG. (A) GFP expression driven by *5'phm*-GAL4 indicates the position of the RG in the whole larva. It is located dorso-anterior to the larval central nervous system. (B) The RG is a composite endocrine organ consisting of three distinct subtissues: the prothoracic gland, the corpus allatum, and the paired corpora cardiaca. Each subtissue synthesizes a different hormone.

Figure 2 Regulation of ecdysteroidogenesis. A huge range of factors influence the ecdysteroidogenic output of the PG cells. PTTH is the major tropic regulator. When PTTH binds its receptor Torso, this activates a Ras-Raf-ERK pathway and a Ca^{2+}-dependent pathway. Other tropic pathways include ILP signaling, TOR signaling, 20E signaling, serotonin signaling, and NO signaling, plus activin upregulates InR and Torso. JH and 20E can both downregulate ecdysteroidogenesis. Our knowledge of these regulatory signaling pathways comes from studies in lepidoptera only (*italic text*), or from studies in both lepidoptera and diptera (bold text). PTTH, prothoracicotropic hormone; Cam-AdCyc, calmodulin-adenylase cyclase; NO, nitric oxide; JH, juvenile hormone; 20E, 20-hydroxyecdysone; ILP, insulin-like peptide. (Adapted from Marchal *et al.* 2010; Yamanaka *et al.* 2013).

20E to initiate the changes in gene expression required for metamorphosis (reviewed in Berger and Dubrovsky 2005; Rewitz *et al.* 2013).

The third and smallest RG subtissues are the corpora cardiaca (CC), found paired at the base of each RG lobe (King *et al.* 1966). The CC cells are heavily involved in glucose regulation, being the primary site of adipokinetic hormone (Akh) production in the larva (Kim and Rulifson 2004). Akh is a peptide hormone that is functionally equivalent to mammalian glucagon; it is active in the larval fat body, where it triggers mobilization of lipids and carbohydrates into the hemolymph (Bharucha *et al.* 2008).

This transcriptome analysis of wandering third instar larvae encompasses all three RG subtissues. There are a number of questions surrounding the role of the RG subtissues that are addressed. First, there are a number of genes in the ecdysteroidogenesis pathway that are yet to be identified [known as the "Black Box" genes (reviewed in Grieneisen 1994; Rewitz *et al.* 2006; Niwa and Niwa 2014)]. Many of the known ecdysteroidogenesis reactions are catalyzed by cytochrome P450s (CYPs) (Chavez *et al.* 2000; Warren *et al.* 2002, 2004; Petryk *et al.* 2003; Niwa *et al.* 2004; Ono *et al.* 2006) so CYPs expressed in the RG would be candidate Black Box genes. Second, this transcriptomic analysis provides the opportunity to clarify ecdysteroidogenesis regulatory pathways of *D. melanogaster*. A multitude of tropic and static factors bind in the PG cells to provide tight temporal control of ecdysteroidogenesis (see Figure 2) (reviewed in Huang *et al.* 2008; Marchal *et al.* 2010; and Yamanaka *et al.* 2013); however, some components within these pathways have been investigated only in lepidoptera. Third, while ecdysteroidogenesis is recognized as the primary function of the PG, there is ultrastructural evidence from *D. melanogaster* that suggests the PG cells may be performing other roles, particularly in late larval development before the PG cells regress (Dai and Gilbert 1991).

Using RNA-seq, we have gained a fresh insight into the range of genes expressed in the *D. melanogaster* wandering third instar RG. We identified 2462 genes significantly enriched in the RG relative to the CNS. As RG-enriched genes included those involved in hormone synthesis, but there were also genes involved in the immune response, and many
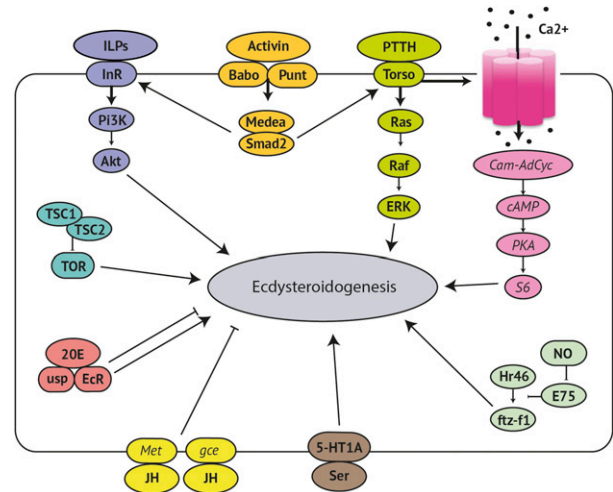
(1310) uncharacterized genes. One of the RG-enriched CYP genes, *Cyp6u1*, was knocked down in the PG using RNA interference (RNAi). This produced a lethal low ecdysone phenotype, flagging a critical role for this gene in development. We also provide a comparison between our data and a recently published RG resource obtained by microarray (Ou *et al.* 2016). As the first complete RG transcriptome, examination of the many highly enriched genes identified in this study may ultimately reveal entirely novel function(s) of the RG subtissues.

MATERIALS AND METHODS

Dissection, RNA isolation and sequencing

RGs were dissected from wandering third instar larvae for two wild-type strains: the reference genome strain y[1]; cn[1] bw[1] sp[1] (Cel) and Armenia[14] (A14) (Perry *et al.* 2012) (all fly stocks listed in Supplemental Material, Table S1). Dissections were performed in 100% PBS in batches of 10–40 at a time, then pooled into three biological replicates for both Cel and A14; ~80 RGs were pooled to provide the ~1 μg of RNA required for sequencing. Total RNA was extracted using the Reliaprep RNA Cell Miniprep System (Promega), then stored at −80°. Total RNA was quality assessed using the 2100 Bioanalyzer (Agilent Technologies), polyA enriched, cDNA libraries prepared, and 100 bp paired-end RNA-seq performed on the Illumina HiSeq2000 system (Australian Genome Research Facility, AGRF). In addition to the reads obtained from the six RG samples, duplicate RNA-seq reads for the Oregon-R wandering third instar CNS were downloaded from the modMINE database (accession: SRX029398) (Contrino *et al.* 2012). These reads were downloaded in SRA (short read archive) format, and converted to paired end fastq format using the *fastq-dump* utility included in the NCBI SRA toolkit.

Transcriptome construction and analysis

Paired fastq sequencing reads were aligned to the annotated *D. melanogaster* reference genome (BDGP release 5) using TopHat 2.0.13 (Trapnell *et al.* 2012). Expression levels were quantified as FPKM (fragments per kilobase of transcript per million fragments mapped), and differential expression was calculated using Cufflinks 2.2.1 (Trapnell *et al.* 2012), with options to enable reference annotation based transcript assembly (–g), fragment bias correction (–b), multi-read correction (–u), and increased maximum fragment alignment (–max-bundle-frags). Quality of the samples was confirmed by examining the dataset for expression of transcripts that would indicate contamination (see Figure S1). Gene ontology enrichment analysis was carried out using the Functional Annotation Clustering tool from the Database for Annotation, Visualization and Integrated Discovery (DAVID 6.7) (Huang *et al.* 2009). Clusters with enrichment scores of at least 1.3 (equivalent to nonlog $P < 0.05$) were further investigated. Secretome analysis was carried out using Signal P 4.1 (Petersen *et al.* 2011). A D-score of ≥ 0.45 was used as the cutoff value to discriminate signal peptides from nonsignal peptides. Flybase (St Pierre *et al.* 2014) was used to investigate gene function.

RNAi gene knockdown

Using available UAS-dsRNA lines and DNA constructs from the Vienna Drosophila RNAi Center (VDRC) (Dietzl *et al.* 2007), select RG-enriched CYPs (*Cyp4g1*, *Cyp4d2*, *Cyp6g2*, *Cyp6u1*, and *Cyp6v1*) were knocked down. Five UAS-RNAi males were crossed to five virgin GAL4 females to achieve ubiquitous knockdown (*tubulin*-GAL4) and RG-specific knockdowns (5′*phm*-GAL4, PG; 5′*6g2*-GAL4, CA; *Akh*-GAL4, CC). All crosses were conducted at 22° with four replicates. Significance was calculated using a Student's *t*-test. Where lethality was observed, crosses were also conducted in cages and 50 first instar larvae were picked into vials ($n = 250$). To monitor developmental timing, 10 first instar larvae were picked onto grape juice plates ($n > 40$) and developmental stages scored daily. All fly stocks used are listed in Table S1.

qPCR was used to validate RNAi knockdown of RG-enriched CYPs (*Cyp4g1*, *Cyp4d2*, *Cyp6g2*, *Cyp6u1*, and *Cyp6v1*), and to measure expression of the JH-regulated gene *Kruppel homolog 1* (*Kr-h1*) in *Cyp6g2* RNAi flies. Virgin *tubulin*-GAL4 females were crossed to males carrying each UAS-dsRNA construct and males from each of the control lines w[1118] and 60100. For each of three biological samples, 10 whole second instar larvae were collected, and RNA was isolated using either the Reliaprep RNA Cell Miniprep System (Promega) (*Cyp4g1*, *Cyp4d2*, *Cyp6u1*, and *Cyp6v1*) or using TRIzol Reagent (Thermo Fisher Scientific) (*Cyp6g2*). RNA concentration was measured using the Qubit Fluorometer. cDNA was synthesized from 440 ng RNA using the SuperScriptIII Reverse Transcriptase kit (Invitrogen). qPCR reactions for each biological sample were carried out in triplicate using a Quanitfast SYBR Green PCR kit (Qiagen) on the CFX384 Touch Real-Time PCR Detection System (Bio-Rad). The amount of target RNA was normalized to the endogenous controls *RpL32* and *CG13220* (Van Hiel *et al.* 2009) (*Cyp4g1*, *Cyp4d2*, *Cyp6u1*, and *Cyp6v1*) or *RpL11* and *RpL24* (*Cyp6g2* and *Kr-h1*). mRNA levels were compared between samples using the $\Delta\Delta^{-Ct}$ method (Bustin *et al.* 2009) using qbase+ software (Biogazelle). All primer sets used are provided in Table S2, the MIQE checklist is provided in Table S3, and qPCR results are in Figure S2.

Ecdysteroid extraction and ELISA

Ecdysteroids were extracted and quantified following a procedure adapted from Yamanaka *et al.* (2015). Ten RG–CNS complexes were dissected and rinsed in PBS, then pooled in 300 μl of methanol on ice.
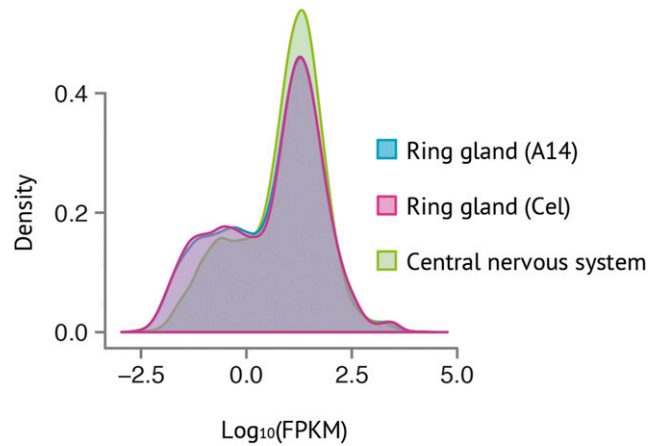

Figure 3 Distribution of FPKM values for all genes in the Armenia[14] RG (blue), the Celera RG (pink), and the Oregon-R central nervous system (green). The distribution is similar for all samples. RG samples have more genes that are very lowly expressed (FPKM < 1), while the CNS has more genes that are lowly ($1 < $ FPKM < 10) to moderately ($10 <$ FPKM < 50) expressed. The image was generated using CummeRbund (Trapnell *et al.* 2012).

The tissue was homogenized by passing through a 23-gauge needle and centrifuged at 4° for 5 min. Supernatants were collected, and the pellet re-extracted with 300 μl methanol. For hemolymph samples, 4 μl hemolymph was collected from 10 larvae, and mixed with 100 μl of methanol on ice. Samples were vortexed and centrifuged at 4° for 5 min. All supernatants were stored at −20° prior to use. Immediately prior to the ELISA, all sample solutions were dried with a SpeedVac concentrator, and dissolved in EIA buffer from the 20-hydroxyecdysone EIA kit (Cayman Chemical). The ELISA assay was performed according to the manufacturer's instructions. Ecdysteroid levels were normalized to the amount of protein in each sample. Protein levels were measured with a Bradford Protein Assay (Bio-Rad) according to the manufacturer's instructions.

Data availability

Strains are available upon request. Raw sequence reads and processed data files, including the table of FPKM estimates output by Cuffdiff, are available from the National Center for Biotechnology Gene Expression Omnibus under the accession number GSE76304.

RESULTS AND DISCUSSION

Gene expression in the third instar larval ring gland

Total RNA was extracted from the RGs of Cel and A14 wandering third instar larvae then submitted for RNA-seq (summarized in Table S4). A total of 188,742,322 reads was generated by 100 bp paired-end sequencing using an Illumina Hiseq2000 at the AGRF. These reads were evenly distributed among the six samples, with the sequencing depth ranging from 28,578,817 to 33,621,275 reads. In addition to the reads obtained from the six RG samples, two replicates of RNA-seq reads for the wandering third instar CNS were downloaded from modMINE (Contrino *et al.* 2012). Given the proximity to the RG, the CNS reads were used to check for any contamination, and for differential gene expression analysis. For all eight samples, overall read alignment rates were very high, ranging from 87.1 to 91.4%. Concordant pair alignment rates were slightly lower, but still well within acceptable limits, ranging from 78.6 to 86.7%.

Table 1 Most highly enriched genes in the RG, sorted by FPKM value

Flybase Symbol	Gene Name	FPKM[a]	Fold Enrichment[a]	GO Term[b]	
				Biological Process	Molecular Function
phm	Phantom	13,305	+113.35	Ecdysone biosynthetic process	Ecdysteroid 25-hydroxylase activity
sad	Shadow	12,617	+161.98	Ecdysone biosynthetic process	Ecdysteroid 2-hydroxylase activity
Npc1a	Niemann-Pick C type 1a	5479	+113.67	Regulation of cholesterol transport	Hedgehog receptor activity
nvd	Neverland	3759	+194.61	Ecdysteroid biosynthetic process	Oxidoreductase activity
CG15919		3706	+3370.16		
CG4408		3221	+123.63	Proteolysis	Metallocarboxypeptidase activity
CG6310		1663	+147.05		
nobo	Noppera-bo	1203	+126.97	Ecdysteroid biosynthetic process	Glutathione transferase activity
Cyp6g2	Cytochrome p450 6g2	992	+145.16	Oxidation-reduction process	Monoxygenase activity
dib	Disembodied	918	+206.62	Ecdysone biosynthetic process	Ecdysteroid 22-hydroxylase activity
CG10337		792	+190.80		
CG9184		598	+152.41		
jhamt	Juvenile hormone acid methyltransferase	587	+407.92	Juvenile hormone biosynthetic process	Juvenile hormone acid methyltransferase activity
CG4822		534	+122.62		Transporter activity
CG6426		524	+130.14	Multicellular organism reproduction	Lysozyme activity
CG13101		430	+202.16		
Tsp42El	Tetraspanin 42El	411	+131.97		
CG2254		392	+107.46	Metabolic process	Oxidoreductase activity
Lectin-galC1	Galactose-specific C-type lectin	191	+161.69	Induction of bacterial agglutination	Galactose binding
tor	Torso	162	+101.70	Metamorphosis	Protein tyrosine kinase activity
CG30471		120	+264.62		Transferase activity
CG40006		111	+235.07	Cell adhesion	
Cyp6a13	Cytochrome p450 6a13	107	+509.06	Defense response to bacterium	Oxidoreductase activity

We have selected GO terms that were most informative for our study, other GO terms for each gene can be found at FlyBase (St Pierre *et al.* 2014).
[a] Only Cel RG data are provided, for A14 data see Table S7.
[b] Regular text = based on experimental evidence, italics = based on predictions or assertions.

Cufflinks (Trapnell *et al.* 2012) was used to calculate the FPKM values. As can be seen in Figure 3, a similar FPKM distribution pattern was found in both RG samples and in the CNS. A large number of genes were very lowly expressed (FPKM < 1), the majority of genes were lowly (1 < FPKM < 10) to moderately expressed (10 < FPKM < 50), and there were fewer genes highly (50 < FPKM < 1000) to extremely highly (FPKM > 1000) expressed (Gelbert and Emmert 2013). Many of the genes in the latter category were ribosomal proteins (see Table S5).

To determine the total number of genes expressed in the RG, a FPKM threshold of one was applied to the dataset (Adrian and Comeron 2013; Graveley *et al.* 2011); 8292 and 8440 genes were expressed in the Cel and A14 RGs, respectively. The expression of 8055 genes was detected in both RG samples (see Table S6 for genotype-dependent RG expression). These 8055 represent 73.7% of all genes expressed in the whole body of wandering third instar larvae [10,926 genes (Daines *et al.* 2011)], a figure comparable to the number of genes expressed in the CNS (8715). Our annotation showed that 57.8% of all genes annotated in the *D. melanogaster* genome (13,918 genes, *Ensembl*, Cunningham *et al.* 2015) were expressed; 50% of genes are typically expressed in other larval tissues (Chintapalli *et al.* 2007).

Of the 8055 RG genes, differential expression analysis revealed that 2462 of these gene transcripts were significantly enriched in both RG samples relative to the CNS. The degree of enrichment exceeded 100-fold for 40 of these RG-enriched gene transcripts (see Table 1 and Table S7). Among these, 20 were genes of unknown function. The values used to calculate differential expression (CNS *vs.* RG) were from the Cel samples. Differential expression analysis using the A14 data provided similar results (see Tables S5–10, S12–13). A notable caveat of using the CNS for differential expression analysis is that transcripts may be reported as RG-enriched when in fact they are CNS-depleted relative to other tissues. This must be considered when interpreting our results.

Ring gland expression of ecdysteroidogenesis genes

Much of what is known about ecdysteroidogenesis comes from a combination of lepidopteran and dipteran studies. This RNA-seq data provides a more complete picture of pathways not fully investigated in *D. melanogaster*. We explored the expression levels of key genes that are either involved in the regulation of ecdysteroidogenesis, or are members of the ecdysteroidogenic pathway (see Table 2 and Table S8).

All genes in the central ecdysteroidogenesis pathway were highly expressed, with the exception of *spook* and *shade*. Low expression of

■ Table 2 Expression of select genes involved in ecdysteroidogenesis

Flybase Symbol	Gene Name	FPKM[a]	Fold Enrichment[a]	q-Value
Ecdysteroidogenic enzymes				
nobo	Noppera-bo	1203	+126.97	<0.001
nvd	Neverland	3759	+194.61	<0.001
spo	Spook	0.6	+15.73	0.3
spok	Spookier	0.0[b]	0	1
sro	Shroud	775	+59.80	<0.001
phm	Phantom	13,305	+113.35	<0.001
dib	Disembodied	918	+206.62	<0.001
sad	Shadow	12,617	+161.98	<0.001
shd	Shade	0.8	+2.68	0.09
Cholesterol homeostasis				
Npc1a	Niemann Pick C type 1a	5479	+113.67	<0.001
Npc2a	Niemann Pick C type 2a	139	+1.01	1
Start1	Start1	2277	+90.48	<0.001
mdy	Midway	129	+26.03	<0.001
PTTH signaling				
tor	Torso	162	+101.70	<0.001
Ras	Ras	97	+1.95	0.006
Raf	Raf	11	−2.11	<0.001
ERK	ERK	0.0[b]	0	1
Cam	Calmodulin	1240	+2.18	<0.001
rut	rutabega	18	−3.16	<0.001
PKA	Protein kinase A	71	−1.90	<0.001
RpS6	Ribosomal protein S6	2528	+1.33	0.05
Hr4	Hormone receptor 4	14	−1.35	0.02
Insulin signaling				
InR	Insulin receptor	12	−1.49	<0.001
Pi3K	Phosphotidylinositol 3 kinase	22	+1.18	0.3
Akt	Akt	50	+1.42	0.003
Activin signaling				
babo	Baboon	47	−1.13	0.4
put	Punt	67	+3.04	<0.001
smad2/smox	Smad on X	40	−2.69	<0.001
Nitric oxide signaling				
E75	Ecdysone-induced protein 75	54	−4.18	<0.001
Hr46	Hormone receptor-like 46	26	+3.07	<0.001
ftz-f1	ftz transcription factor 1	2	−1.97	0.002
TOR signaling				
TSC1	TSC1	20	−1.33	0.03
TSC2/gig	TSC2	17	+1.48	0.02
Tor	Target of rapamycin	23	+1.04	0.8
Serotonin signaling				
5-HT1A	5-hydroxytryptamine (serotonin) receptor 1A	1	−5.70	<0.001
JH signaling				
Met	Methoprene-tolerant	4	−2.90	<0.001
gce	Germ cell-expressed bHLH-PAS	4	−2.23	<0.001
20E signaling				
EcR	Ecdysone receptor	80	+1.59	<0.001
usp	Ultraspiracle	28	−1.93	0.01

[a] Only Cel RG data are provided, for A14 data see Table S8.
[b] Genes located in heterochromatic regions were not included in reference genome. Reads corresponding to these genes were therefore not aligned by Tophat, hence the 0.0 FPKM score.

spook was expected, given that this enzyme is required only during embryonic ecdysteroidogenesis, and not during larval stages (Ono *et al.* 2006). Low expression of *shade* is consistent with ecdysone being activated to 20E in peripheral tissues, and not the PG (Petryk *et al.* 2003). Multiple genes involved in cholesterol homeostasis were highly expressed. Cholesterol is a critical precursor for synthesis of many hormones [reviewed in Edwards and Ericsson (1999)], and the enhanced expression of *Npc1a* and *Start1* suggests that these proteins are likely the primary ER transporters responsible for cholesterol availability in the PG cells.

The enhanced expression of the prothoracicotropic hormone (PTTH) receptor, *torso*, is consistent with PTTH being the primary tropic regulator of ecdysteroidogenesis (McBrayer *et al.* 2007; Rewitz *et al.* 2009). In the tobacco hornworm *Manduca sexta*, it is clear that at least two pathways act downstream of PTTH; the Ras-Raf-ERK pathway is dominant during larval development, then, at metamorphosis, a Ca^{2+} and cAMP-dependent pathway becomes dominant (Rybczynski and Gilbert 2003) (see Figure 2). Until now, little has been noted about the Ca^{2+}- and cAMP-dependent pathway in *D. melanogaster*, aside from Ca^{2+} influx

Cytochrome p450	FPKM[a]	Fold Enrichment[a]	q Value	Annotated Biological Process[b]	Ubiquitous RNAi Knockdown[c]	Clade Stability Across Drosophila Species[d]
phm	13,305	+113.35	<0.001	Ecdysone biosynthetic process	Lethal	Stable
sad	12,617	+161.98	<0.001	Ecdysone biosynthesis process	n/a	Stable
Cyp6g2	992	+145.01	<0.001	*Oxidation-reduction process*	Lethal	Stable
dib	918	+206.62	<0.001	Ecdysone biosynthetic process	n/a	Stable
Cyp6a13	107	+509.06	0.007	Defense response to bacterium	Viable	Gene loss
Cyp6v1	96	+8.42	<0.001	*Oxidation-reduction process*	n/a	Stable
Cyp12e1	70	+11.96	<0.001	*Oxidation-reduction process*	Viable	Gene gain
Cyp310a1	52	+77.94	0.002	Negative regulation of Wnt signaling pathway	n/a	Gene loss
Cyp6u1	37	+3.57	<0.001	*Oxidation-reduction process*	n/a	Stable
Cyp9f2	20	+1.84	<0.001	Wing disc development	Viable	Gene gain
Cyp4g1	19	+2.72	0.08	Lipid metabolic process	Lethal	Stable
Cyp303a1	15	+17.58	<0.001	Sensory organ development	n/a	Stable
Cyp4d2	15	+3.68	<0.001	*Oxidation-reduction process*	Lethal	Gene loss
Cyp6d4	13	+2.36	<0.001	Wing disc development	Viable	Gene gain
Cyp18a1	6	+28.61	<0.001	Ecdysteroid catabolic process	Lethal	Stable

We selected GO terms that were most informative for our study; other GO terms for each gene can be found at FlyBase (St Pierre *et al.* 2014).
[a] Only Cel RG data are provided, for A14 data see Table S9.
[b] Regular text = based on experimental evidence, italics = based on predictions or assertions.
[c] Chung *et al.* (2009), Guittard *et al.* (2011), and Qiu *et al.* 2012.
[d] Good *et al.* (2014).

appearing to be required for ecdysteroidogenesis in dissected *D. melanogaster* RGs (Henrich 1995). Here, the highly enriched expression of *Calmodulin* and *RpS6* suggests that the Ca²⁺- and cAMP-dependent branch of the PTTH pathway may be conserved in the dipteran lineage (Marchal *et al.* 2010; Lin *et al.* 2011). Another possible role for calcium signaling is regulating vesicle-mediated ecdysone release from the PG (Yamanaka *et al.* 2015). The Ca²⁺ channel/s that facilitate these two calcium-dependent pathways are yet to be identified (Fellner *et al.* 2005; Marchal *et al.* 2010), and we have detected at least nine transmembrane calcium transporters (*PMCA*, *Ca-α1T*, *pain*, *Prestin*, *Itp-r83A*, *Cac*, *Ca-α1D*, *Ca-β*, and *trp*) in the transcriptome.

All known key members of the insulin (Colombani *et al.* 2005; Caldwell *et al.* 2005; Mirth *et al.* 2005), activin (Gibbens *et al.* 2011), nitric oxide (Caceres *et al.* 2011), TOR (Layalle *et al.* 2008), and serotonin (Shimada-Niwa and Niwa 2015) pathways were also detected. The JH receptors *Met* and *gce* (Jindra *et al.* 2015) were both present, supporting evidence that JH negatively regulates ecdysone and JH synthesis at the RG (Richard and Gilbert 1991). Both components of the ecdysone receptor heterodimer, *EcR* and *usp*, were also expressed, adding to evidence that 20E is involved in feedback loops in the RG (Koelle *et al.* 1991; Karim and Thummel 1992; Song *et al.* 2003; Moeller *et al.* 2013).

Uncharacterized cytochrome P450s are enriched in the ring gland

CYPs play an important role in the RG tissues, with the most well-known being the Halloween genes involved in ecdysteroidogenesis in the PG (Chavez *et al.* 2000; Warren *et al.* 2002, 2004; Ono *et al.* 2006). All CYPs were extracted from the dataset, and expression levels investigated to identify candidate CYPs that may belong in the Black Box, or be involved in sterol modification. CYPs that were significantly enriched in both RG samples are listed in Table 3 and Table S9. Given that developmental CYPs tend to be more highly conserved and phylogenetically stable than those involved in metabolism, the clade stability for each gene across the phylogeny of 12 *Drosophila* species was noted (Good *et al.* 2014). Any published RNAi lethality phenotypes (Chung *et al.* 2009; Guittard *et al.* 2011; Qiu *et al.* 2012) were also considered.

The most highly expressed CYPs were the known Halloween genes, plus the CA-specific *Cyp6g2*, which may be involved in JH synthesis (Chung *et al.* 2009; Wen *et al.* 2015). These genes all had expression levels >900 FPKM, but no other CYPs had expression levels in this range. Nonetheless, there were some CYPs with relevant features. *Cyp4g1* knockdown is lethal at the pupal stage (Chung *et al.* 2009; Qiu *et al.* 2012), and its closest homolog, *Bombyx mori Cyp4g25*, is induced by PTTH in the PG (Niwa *et al.* 2011). *Cyp4d2* knockdown is also lethal at the pupal stage (Chung *et al.* 2009). A notable exception from the enriched CYPs is *Cyp6t3*. Loss of *Cyp6t3* was previously shown to disrupt ecdysone biosynthesis (Ou *et al.* 2011); however, *Cyp6t3* transcripts were effectively absent from our RG samples (FPKM > 1).

RNAi knockdown of ring gland-enriched cytochrome p450s: To establish whether any of the RG-enriched CYPs play an important role in the RG, we investigated their ubiquitous and RG-specific RNAi knockdown viability. A subset of the enriched CYPs (*Cyp4g1*, *Cyp4d2*, *Cyp6u1*, and *Cyp6v1*) was tested based on expression level, previously reported RNAi lethality (Chung *et al.* 2009; Guittard *et al.* 2011; Qiu *et al.* 2012), and/or the stability of their gene clade (Good *et al.* 2014).

For *Cyp4g1*, 100% pupal lethality was observed for ubiquitous knockdown, as previously reported by Chung *et al.* (2009) and Qiu *et al.* (2012) (*n* > 250) (see Figure 4, A and B, and Figure S3). Tissue-specific knockdown of *Cyp4g1* in each of the RG subtissues had no effect on viability. We conclude that *Cyp4g1* does not play an essential developmental role in the RG, and attribute the ubiquitous knockdown lethality to *Cyp4g1*'s known role in cuticular hydrocarbon synthesis in the oenocytes (Qiu *et al.* 2012).

For *Cyp4d2*, ubiquitous RNAi resulted in 96% lethality (*n* > 250) (see Figure 4, A and B). This is consistent with the 100% pupal lethality observed by Chung *et al.* (2009), and with the EMS-induced K350X mutation that causes lethality (Haelterman *et al.* 2014). The 4% of individuals that survived to adulthood all had asymmetrical melanization on their wings (see Figure 4D). This phenotype is reminiscent of the wing patterning of *Drosophila suzukii*, and motivated us to look for this gene in the *D. suzukii* genome sequence. Interestingly, *Cyp4d2* is missing from the current *D. suzukii* genome assembly, although a short
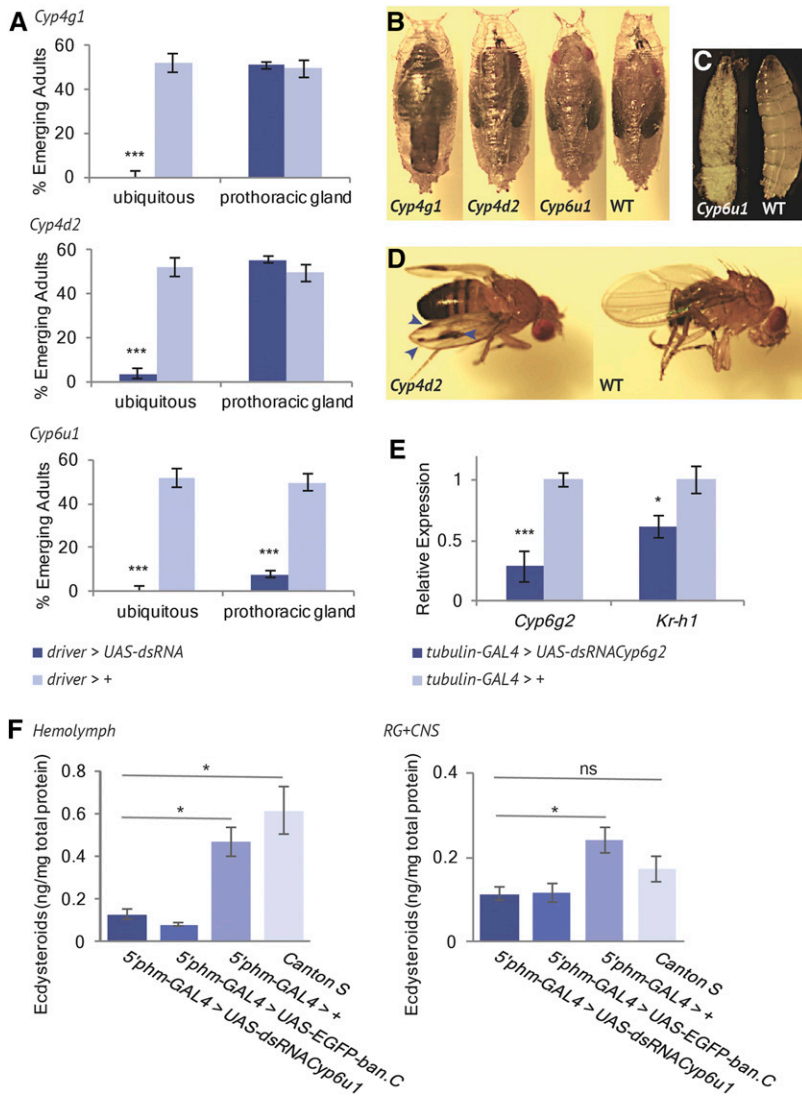
Figure 4 RNAi knockdown of RG-enriched cytochrome p450s. (A) Cytochrome p450s were knocked down ubiquitously (*tubulin*-GAL4), and with a PG-specific driver (5′*phm*-GAL4), and the resulting progeny scored for viability ($n > 250$). Each bar represents mean ± SEM. Significance was calculated using a Student's *t*-test (*** $P < 0.0001$). (B, C) Representative pupae and larvae at the time of lethality and equivalent wild-type individuals. Ubiquitous knockdown is shown for *Cyp4g1* and *Cyp4d2*. PG-specific knockdown is shown for *Cyp6u1*. (D) Adults that survived ubiquitous *Cyp4d2* knockdown had variable, asymmetrical melanization on their wings (arrows). (E) qPCR reveals significantly lowered levels of *Kr-h1*, a juvenile hormone primary response gene, and *Cyp6g2* transcripts in *Cyp6g2* knockdown larvae. Significance was calculated using a Student's *t*-test (* $P < 0.05$, *** $P < 0.0001$). (F) Quantity of ecdysteroids in the hemolymph and RG-CNS complexes of wandering third instar larvae is severely reduced in *Cyp6u1* PG-RNAi larvae. Bars represent the mean ± SEM of three independent samples. Significance was calculated using a Student's *t*-test (* $P < 0.05$).

stretch of missing bases provides the possibility that the gene, by co-incidence, may be present in the genome but missing in the assembly (see Figure S4). The absence of *Cyp4d2* in the *D. suzukii* transcriptome datasets (male and female) in which genes such as the Halloween CYPs are present, adds support to the proposition that *Cyp4d2* has genuinely been lost in *D. suzukii*. Wing spots in the Oriental species of the *melanogaster* species group have been gained and lost multiple times (Kopp and True 2002), and multiple loci determine their presence and size (Yeh and True 2014). *D. biarmes*, a species closely related to *D. suzukii*, has wing spots, and its genome does contain intact *Cyp4d2* coding sequence, although whether it is expressed in the relevant tissues is unknown. Thus, unexpectedly, we have stumbled on a gene that may be considered as a candidate affecting wing spots in the Oriental *Drosophila* lineage. Tissue-specific knockdown of *Cyp4d2* in each of the RG subtissues had no effect on viability (see Figure 4A and Figure S3).

For *Cyp6u1*, ubiquitous knockdown was 100% lethal (see Figure 4A) ($n > 250$), with most lethality occurring at the first larval instar (32%), second larval instar (10%), and third larval instar (54%) ($n = 50$) (see Figure 5A). Larvae often died during or shortly after molting. PG-specific knockdown of *Cyp6u1* was 92% lethal (see Figure 4, A–C), with lethality occurring at the first larval instar (18%), second larval instar (16%), third larval instar (26%), pupation (4%), and eclo-

sion (34%) ($n = 50$) (see Figure 5B). Once again, larval lethality was often associated with incomplete moulting. This result is the first reported evidence that *Cyp6u1* may play a critical developmental role in the PG. We also quantified ecdysteroid levels in the hemolymph and RG-CNS complexes of wandering third instar *Cyp6u1* PG-specific RNAi larvae. In both the hemolymph and RG-CNS, *Cyp6u1* RNAi larvae had severely reduced ecdysteroid levels compared to the GAL4-only control, and comparable ecdysteroid levels to another ec-dysone deficient line (5′*phm*-GAL4 > UAS-EGFP-ban.C; Boulan *et al.* 2013) (see Figure 4F). These low ecdysteroid levels, combined with the heterochronic lethality and incomplete molting, provide strong evidence that *Cyp6u1* may have a role in ecdysteroidogenesis, possibly in the Black Box. While the known Halloween genes all share a characteristic embryonic lethal phenotype for complete loss-of-function (Rewitz *et al.* 2006; Niwa and Niwa 2014), RNAi knockdown of Halloween genes is less severe. Individuals with PG-specific knock-down of *phm*, *dib*, or *nobo* may die as larvae or pupae (Ou *et al.* 2011; Enya *et al.* 2014). Other non-Halloween ecdysteroidogenesis genes also have similar heterochronic lethality upon PG-specific RNAi knock-down (Yoshiyama *et al.* 2006; Niwa *et al.* 2011; Ou *et al.* 2011). So far, all of our evidence suggests that *Cyp6u1* is involved in ecdysteroido-genesis, but a null allele will reveal whether complete loss-of-function is
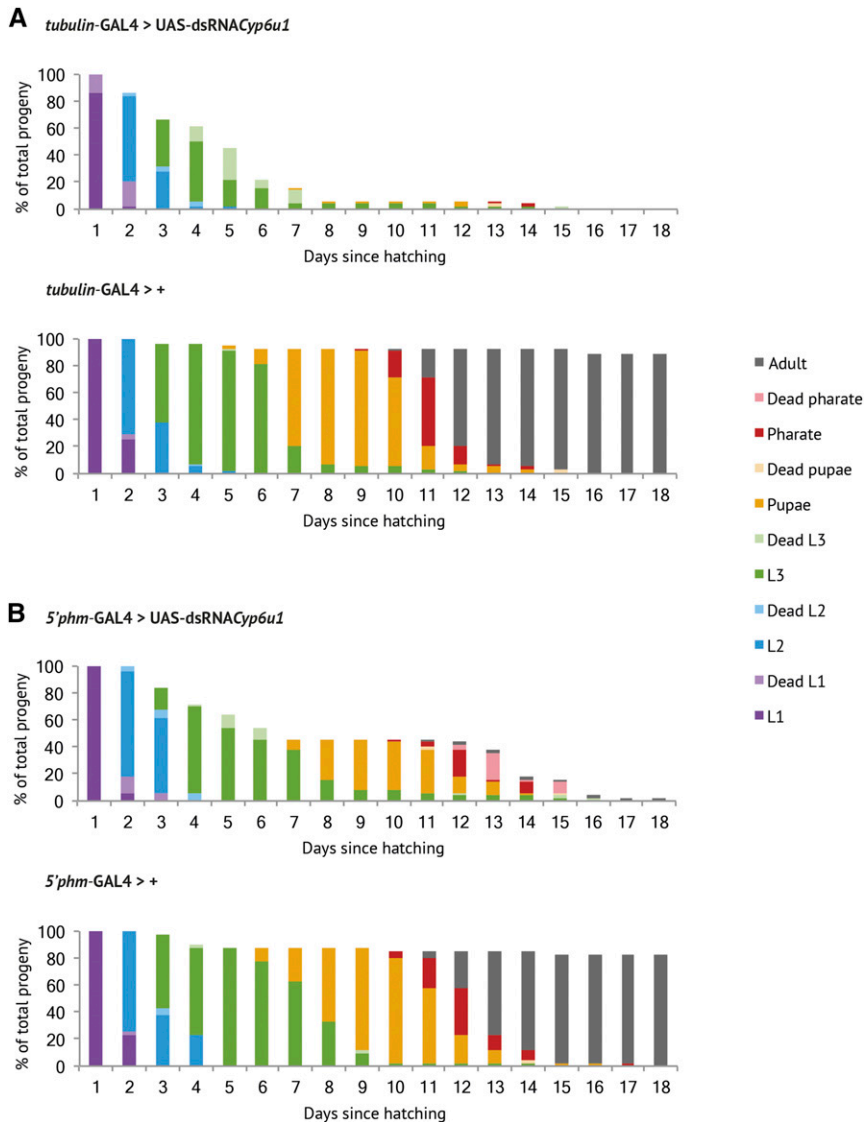
Figure 5 RNAi knockdown of *Cyp6u1* results in lethality throughout larval and pupal development. The percentage at each developmental stage per day posthatching ($n > 40$) is shown. Each color represents a different developmental stage, with lighter shades representing dead individuals. (A) For ubiquitous knockdown, lethality was observed at the first larval instar (32%), second larval instar (10%), and third larval instar (32%). (B) For PG-specific knockdown, lethality was observed at the first larval instar (18%), second larval instar (16%), third larval instar (26%), pupation (4%), and eclosion (34%).

embryonic lethal, and thus whether *Cyp6u1* achieves the status of Halloween gene.

Tissue-specific knockdown of *Cyp6u1* in the CA and CC did not result in any phenotypes (see Figure S3).

For *Cyp6v1*, all ubiquitous and RG-specific knockdowns were viable ($n > 500$) (see Figure S3). qPCR indicates that *Cyp6v1* expression was actually increased in the *tubulin*-GAL4; UAS-*dsRNA-Cyp6v1* strain relative to the w[1118]; *tubulin*-GAL4 background control (see Figure S2). Thus, the RNAi knockdown was ineffective, and we are unable to report a conclusive knockdown phenotype for this gene.

Expression of a JH-regulated gene is decreased by Cyp6g2 RNAi: Previous work has shown that *Cyp6g2* is the only CYP expressed in the CA, and that RNAi knockdown of *Cyp6g2* is pupal lethal (Chung *et al.* 2009). This makes *Cyp6g2* a promising candidate for the JH synthesis pathway. Using qPCR, we observed significantly reduced expression levels of *Kr-h1*, a JH primary response gene (Minakuchi *et al.* 2008; Abdou *et al.* 2011; He *et al.* 2014), in *Cyp6g2* RNAi larvae compared to GAL4-only controls (see Figure 4E). This suggests a decrease in JH titers in *Cyp6g2* RNAi larvae, and strengthens the evidence for *Cyp6g2*'s involvement in JH synthesis.

Gene ontology enrichment analysis

Throughout the first, second, and most of the third, larval instar stages, the PG cells have a very well developed smooth endoplasmic reticulum (ER) (Dai and Gilbert 1991). This is typical of cells involved in steroid synthesis (De Loof 2008). From the wandering third instar stage, however, the smooth ER begins to regress, and the rough ER becomes abundant. This is typical of cells involved in protein secretion, suggesting the PGs may have an additional secretory role in the lead up to pupation. In this study, we have performed gene ontology enrichment analysis to uncover any genes that may be involved in any nonsteroidogenic functions. A subset of 288 transcripts was selected for this analysis using the following criteria: (1) at least 10-fold enrichment in both RG samples relative to the CNS, and (2) statistically significant enrichment in both RG samples relative to the CNS genes (see Table S10). With these 288 transcripts, we used DAVID Functional Annotation Clustering (Huang *et al.* 2009) to identify three biological processes: lipid biosynthesis, fatty acid metabolism, and immune response (see Table 4).

The lipid biosynthesis cluster (18 genes) is the most significantly enriched, owing to the abundance of genes involved in ecdysone biosynthesis (*phm*, *sad*, *nvd*, and *dib*), cholesterol homeostasis (*Npc1a*,

■ **Table 4 Top ranked biological processes represented by RG-enriched transcripts**

Annotation Cluster	Flybase Symbol	Gene Name
Enrichment score: 2.76		
GO:0008610 - lipid biosynthetic process	phm	Phantom
GO:0006694 - steroid biosynthetic process	sad	Shadow
GO:0008202 - steroid metabolic process	Npc1a	Niemann-Pick type c 1 a
GO:0034754 - cellular hormone metabolic process	nvd	Neverland
GO:0042446 - hormone biosynthetic process	Start1	Start1
GO:0042445 - hormone metabolic process	dib	Disembodied
GO:0010817 - regulation of hormone levels	jhamt	Juvenile hormone acid methyltransferase
GO:0042181 - ketone biosynthetic process	hmas	HMG coenzyme A synthase
GO:0045456 - ecdysteroid biosynthetic process	CG8306	
GO:0045455 - ecdysteroid metabolic process	CG8239	
GO:0016125 - sterol metabolic process	mdy	Midway
GO:0006697 - ecdysone biosynthetic process	Pgd	Phosphogluconate dehydrogenase
GO:0016126 - sterol biosynthetic process	CG10932	
GO:0008205 - ecdysone metabolic process	CG8630	
GO:0019748 - secondary metabolic process	jheh1	Juvenile hormone epoxide hydrolase 1
	yellow-f	yellow-f
	CG17928	
	Cyp18a1	Cytochrome p450 18a1
Enrichment score: 1.68		
GO:0006631 - fatty acid metabolic process	CG8306	
GO:0006633 - fatty acid biosynthetic process	CG10932	
GO:0016053 - organic acid biosynthetic process	CG8630	
GO:0046394 - carboxylic acid biosynthetic process	CG3267	
	CG17928	
	tan	tan
Enrichment score: 1.55		
GO:0019730 - antimicrobial humoral response	Thor	Thor
GO:0019731 - antibacterial humoral response	He	Hemese
GO:0009617 - response to bacterium	TepI	Thioester-containing protein I
GO:0006959 - humoral immune response	CG16799	
GO:0006955 - immune response	Drs	Drosomycin
GO:0042742 - defense response to bacterium	pirk	poor imd response upon knock-in
GO:0006952 - defense response	LysS	Lysozyme S
	psh	Persephone
	TepII	Thioester-containing protein II

Gene ontology enrichment analysis was carried out using the Functional Annotation Clustering tool of (DAVID 6.7) (Huang *et al.* 2009). Clusters with enrichment scores >1.3 (equivalent to nonlog $P < 0.05$) are shown.

Start1, and *mdy*), ecdysone inactivation (*Cyp18a1*), and JH biosynthesis (*jhamt*, *hmgs*, *CG8239*, and *jheh1*). This cluster also, together with the fatty acid metabolism cluster (six genes), reveals a subset of uncharacterized genes not previously associated with any RG subtissues (*CG8360*, *CG10932*, *CG8630*, *CG17928*, and *CG3267*). These uncharacterized genes are bioinformatically predicted to modify fatty acids via branching, desaturation, or elongation. Enrichment of these genes may be associated with energy production or cholesterol storage. Another hypothesis is that the PG may use fatty acid deposits as an indicator of nutritional status to regulate ecdysteroidogenesis (Niwa *et al.* 2011). As a predicted acetoacetyl-CoA thiolase, *CG10932* may have a role in the mevalonate pathway upstream of JH biosynthesis in the CA (Bellés *et al.* 2005).

The immune response cluster (nine genes) was an unexpected finding. This cluster includes genes that actively fight microbial infection, specifically an antifungal peptide (*Drs*), and two antibacterial peptides (*LysS*, *CG16799*), plus genes that regulate the immune response. In *D. melanogaster*, the immune response is primarily orchestrated by the fat body and the hemocytes [reviewed in Hoffmann (2003)]. The cells of the fat body synthesize and secrete antimicrobial peptides upon activation of the Toll and Imd pathways (Lemaitre *et al.* 1995, 1996). The hemocytes, on the other hand, primarily participate in cellular responses such as phagocytosis, melanization, and encapsulation of parasites (Rizki and Rizki 1984), but are also capable of antimicrobial peptide production (Samakovlis *et al.* 1990). Based on this transcriptome, it is possible that the RG may be a third contributor to the immune response. The level of enrichment of immune response genes observed here would only be explained by RG expression, as we did not detect sufficient levels of fat body or hemolymph contamination (see Figure S1). In addition, we verified RG expression of a GFP-tagged immune response gene, *TepII* (see Figure S5) (Nagarkar-Jaiswal *et al.* 2015). While the *D. melanogaster* RG has not been previously associated with the immune response, proteomic analysis in the PG of the desert locust *Schistocerca gregaria* has uncovered a number of proteins involved in defense (Boerjan *et al.* 2012).

Ou *et al.* (2016) performed gene ontology enrichment analysis on an array-based RG expression dataset. They too identified "hormone biosynthesis" as a significantly enriched term; however, "immune response" and "fatty acid metabolism" were absent from their results. Inspection of their 208 RG-enriched genes reveals that only 107 were significantly enriched in our RG samples, while 65 were significantly depleted in our RG samples or had similar expression levels to the CNS (see Table S11). We attribute these differences in enrichment, and consequent differences in gene ontology results, to at least two factors;

Flybase Symbol	Gene Name	FPKM[a]
CG4572		535
Jon99Cii	Jonah 99Cii	108
CG33465		64
CG33460		63
CG9372		46
CG4259		39
CG15046		34
CG10663		22
CG10232		21
CG4793		20
CG4927		18
CG4386		18
Jon99Fii	Jonah 99Fii	16
CG10764		15
Jon25Biii	Jonah 25Biii	12
CG3355		11
Jon99Fi	Jonah 99Fi	11
CG33225		11
CG33461		9
Jon66Cii	Jonah 66Cii	7
CG8738		5
psh	Persephone	4

[a] Only Cel RG data are provided, for A14 data see Table S12.

(1) the array-based subset combines four different timepoints throughout the third instar stage, so there will be transcripts specific to earlier timepoints that were not enriched in our wandering third instar samples, and (2) differential expression in the array-based dataset was calculated using whole body expression data, so relative enrichment values will differ to those calculated against CNS expression data.

Secretome analysis of RG-enriched genes

Ultrastructural analysis of the PG cells in *D. melanogaster* has previously revealed a well-developed ER and Golgi, suggesting the PG may have a major role in protein secretion (Dai and Gilbert 1991). To identify genes containing an *N*-terminal signal peptide, the amino acid sequences of all 288 genes enriched at least 10-fold in the RG were sub-

mitted to Signal P (Petersen *et al.* 2011). Of these genes, 112 received a D-score over 0.45, and their products are therefore predicted to enter the secretory pathway, where they will either be retained at the ER, transported to the plasma membrane, or secreted from the cell (see Table S10).

The most abundant class of signal peptide-containing genes are the serine proteases (22/112 genes; 20%) (see Table 5 and Table S12). Secretion of serine proteases into the hemolymph typically initiates proteolytic cascades that then induce various innate immune responses, including melanization (Tang *et al.* 2006) and antimicrobial peptide synthesis (Ligoxygakis *et al.* 2002). A number of these RG-enriched serine proteases are known to be upregulated in response to parasitic, fungal, and bacterial infection (*Jon99Fi*, *Jon25Biii*, *CG9372*, and *CG15046*, *psh*) (Shah *et al.* 2008). There were also 26 uncharacterized genes highlighted by our analysis. *CG4408*, *CG14075*, and *CG11370* are of particular interest as they are expressed very highly, comparable to the Halloween genes *nvd*, *nobo*, and *dib* (Chavez *et al.* 2000; Yoshiyama *et al.* 2006; Enya *et al.* 2014) (see Table 1). These uncharacterized genes may represent some of the most important secreted products in the RG.

RG expression of immune response genes

Given the prevalence of immune response genes and serine proteases among the 288 RG-enriched genes, the RG expression levels of other key genes in the *D. melanogaster* immune system was investigated. These include genes in the two primary innate immune response pathways: the Toll pathway and the Imd pathway (see Table 6 and Table S13) [reviewed in Hoffmann (2003)]. Four of the seven genes in the Toll pathway were significantly enriched in the RG (*Myd88*, *Cactus*, *Dif*, and *Drs*). A Toll receptor (*Toll*) was expressed in both the Cel RG and the A14 RG but was significantly enriched only in the A14 RG. The Toll pathway is involved in defense against fungi and gram-positive bacteria, and activation of this pathway leads to expression of antimicrobial peptides such as drosomycin (Lemaitre *et al.* 1996). The enrichment of these Toll pathway genes suggests that the RG may have the capacity to detect fungal and gram-positive infections, and possibly contribute to the immune response by expressing antimicrobial peptides.

Five of the nine genes in the Imd pathway were significantly enriched in the RG (*PGRP-LC*, *Dredd*, *Tak1*, *ird5*, and *Rel*). This pathway is

■ **Table 6 RG expression of key genes in the immune response pathways**

Flybase Symbol	Gene Name	FPKM[a]	Fold Enrichment[a]	q-Value
Toll Pathway				
Tl	Toll	26 (62[b])	−1.46 (+1.64[b])	<0.001
Myd88	Myd88	15	+1.74	<0.001
pll	Pelle	16	+1.66	0.2
tub	Tube	27	−1.19	0.2
cact	Cactus	97	+1.80	<0.001
Dif	Dorsal-related immunity factor	26	+2.71	<0.001
Drs	Drosomycin	31	+10.77	0.001
Imd Pathway				
PGRP-LC	Peptidoglycan recognition protein LC	9	+5.43	<0.001
imd	Immune deficiency	23	+1.86	0.5
Fadd	Fas-associated death domain ortholog	15	+3.06	0.1
Dredd	Death related ced-3	40	+3.74	<0.001
Tak1	TGF-β activated kinase 1	27	−1.38	0.01
key	Kenny	34	−1.19	0.3
ird5	Immune response deficient 5	16	+4.85	<0.001
Rel	Relish	30	+2.07	<0.001
DptB	Diptericin	3.5	+9.32	0.2

[a] Unless otherwise stated, only Cel RG data are provided. For A14 data see Table S13.
[b] Cel and A14 results were significantly different, therefore A14 data are provided in parentheses.

involved in defense against gram-negative bacteria, and its activation leads to expression of antimicrobial peptides such a diptericin (Lemaitre *et al.* 1995, 1996). The enrichment of these Imd pathway genes suggests that the RG may also be able to detect, and possibly respond to, gram-negative bacterial infections. The enrichment of these Toll and Imd pathway genes could be explained if the PG is able to use the immune status of the larva as an added level of regulation of ecdysteroidogenesis. Given that infection delays pupation (Olcott *et al.* 2010), we suggest that the PG may be able to detect an infection and then, potentially via the Toll and/or Imd pathways, directly or indirectly downregulate Halloween genes to postpone metamorphosis.

Conclusion

This transcriptome has provided a fascinating snapshot of the diversity of developmental signaling occurring in the *D. melanogaster* third instar RG. We discovered a strong enrichment of gene pathways involved in two processes not previously associated with the *D. melanogaster* RG; immune response and fatty acid metabolism. We identified a set of enriched CYPs, at least two of which appear to be performing an essential developmental role in the RG. Furthermore, we uncovered a surplus of unnamed genes that are highly enriched, and whose characterization may help complete the ecdysone biosynthesis pathway and may even reveal additional unknown processes in the RG. Much of this transcriptome still remains to be explored. As the first complete *D. melanogaster* RG transcriptome, we hope this resource will fuel further investigations into the RG, and its broader role in governing insect development.

LITERATURE CITED

Abdou, M. A., Q. He, D. Wen, O. Zyaan, J. Wang *et al.*, 2011 *Drosophila* Met and Gce are partially redundant in transducing juvenile hormone action. Insect Biochem. Mol. Biol. 41: 938–945.

Adrian, A. B., and J. M. Comeron, 2013 The *Drosophila* early ovarian transcriptome provides insight to the molecular causes of recombination rate variation across genomes. BMC Genomics 14: 794.

Baehrecke, E. H., 1996 Ecdysone signaling cascade and regulation of *Drosophila* metamorphosis. Arch. Insect Biochem. Physiol. 33: 231–244.

Bellés, X., D. Martín, and M.-D. Piulachs, 2005 The mevalonate pathway and the synthesis of juvenile hormone in insects. Annu. Rev. Entomol. 50: 181–199.

Berger, E. M., and E. B. Dubrovsky, 2005 Juvenile hormone molecular actions and interactions during development of *Drosophila melanogaster*. Vitam. Horm. 73: 175–215.

Bharucha, K. N., P. Tarr, and S. L. Zipursky, 2008 A glucagon-like endocrine pathway in *Drosophila* modulates both lipid and carbohydrate homeostasis. J. Exp. Biol. 211: 3103–3110.

Boerjan, B., K. Vandingenen, A. De Loof, and L. Schoofs, 2012 In search for non-steroidogenic functions of the prothoracic glands of the desert locust, *Schistocerca gregaria*: a peptidomic and proteomic approach. Peptides 34: 57–64.

Boulan, L., D. Martín, and M. Milán, 2013 *bantam* miRNA promotes systemic growth by connecting insulin signaling and ecdysone production. Curr. Biol. 23: 473–478.

Bownes, M., and H. Rembold, 1987 The titer of juvenile hormone during the pupal and adult stages of the life-cycle of *Drosophila melanogaster*. Eur. J. Biochem. 164: 709–712.

Bustin, S. A., V. Benes, J. A. Garson, J. Hellemans, J. Huggett *et al.*, 2009 The MIQE Guidelines: minimum information for publication of quantitative real-time PCR experiments. Clin. Chem. 55: 611–622.

Caceres, L., A. S. Necakov, C. Schwartz, S. Kimber, I. J. H. Roberts *et al.*, 2011 Nitric oxide coordinates metabolism, growth, and development via the nuclear receptor E75. Genes Dev. 25: 1476–1485.

Caldwell, P., M. Walkiewicz, and M. Stern, 2005 Ras activity in the *Drosophila* prothoracic gland regulates body size and developmental rate via ecdysone release. Curr. Biol. 15: 1785–1795.

Chavez, V., G. Marques, J. Delbecque, K. Kobayashi, M. Hollingsworth *et al.*, 2000 The *Drosophila disembodied* gene controls late embryonic morphogenesis and codes for a cytochrome P450 enzyme that regulates embryonic ecdysone levels. Development 127: 4115–4126.

Chintapalli, V. R., J. Wang, and J. A. T. Dow, 2007 Using FlyAtlas to identify better *Drosophila melanogaster* models of human disease. Nat. Genet. 39: 715–720.

Chung, H., T. Sztal, S. Pasricha, M. Sridhar, P. Batterham *et al.*, 2009 Characterization of *Drosophila melanogaster* cytochrome P450 genes. Proc. Natl. Acad. Sci. USA 106: 5731–5736.

Colombani, J., L. Bianchini, S. Layalle, E. Pondeville, C. Dauphin-Villemant *et al.*, 2005 Antagonistic actions of ecdysone and insulins determine final size in *Drosophila*. Science 310: 667–670.

Contrino, S., R. N. Smith, D. Butano, A. Carr, F. Hu *et al.*, 2012 modMine: flexible access to modENCODE data. Nucleic Acids Res. 40: D1082–D1088.

Cunningham, F., M. R. Amode, D. Barrell, K. Beal, K. Billis *et al.*, 2015 Ensembl 2015. Nucleic Acids Res. 43: D662–D669.

Dai, J. D., and L. I. Gilbert, 1991 Metamorphosis of the corpus allatum and degeneration of the prothoracic glands during the larval-pupal-adult transformation of *Drosophila melanogaster*: a cytophysiological analysis of the ring gland. Dev. Biol. 144: 309–326.

Daines, B., H. Wang, L. Wang, Y. Li, Y. Han *et al.*, 2011 The *Drosophila melanogaster* transcriptome by paired-end RNA sequencing. Genome Res. 21: 315–324.

De Loof, A., 2008 Ecdysteroids, juvenile hormone and insect neuropeptides: recent successes and remaining major challenges. Gen. Comp. Endocrinol. 155: 3–13.

Dietzl, G., D. Chen, F. Schnorrer, K. C. Su, Y. Barinova *et al.*, 2007 A genome-wide transgenic RNAi library for conditional gene inactivation in *Drosophila*. Nature 448: 151–156.

Edwards, P. A., and J. Ericsson, 1999 Sterols and isoprenoids: signaling molecules derived from the cholesterol biosynthetic pathway. Annu. Rev. Biochem. 68: 157–185.

Enya, S., T. Ameku, F. Igarashi, M. Iga, H. Kataoka *et al.*, 2014 A Halloween gene *noppera-bo* encodes a glutathione S-transferase essential for ecdysteroid biosynthesis via regulating the behaviour of cholesterol in *Drosophila*. Sci. Rep. 4: 6586.

Fellner, S., R. Rybczynski, and L. Gilbert, 2005 Ca^{2+} signaling in prothoracicotropic hormone-stimulated prothoracic gland cells of *Manduca sexta*: evidence for mobilization and entry mechanisms. Insect Biochem. Mol. Biol. 35: 263–275.

Gelbert, W. M. and D. B. Emmert, 2013 Flybase high throughput expression pattern data. Available at: http://flybase.org/reports/FBrf0221009.html. Accessed: November 1st, 2015

Gibbens, Y. Y., J. T. Warren, L. I. Gilbert, and M. B. O'Connor, 2011 Neuroendocrine regulation of *Drosophila* metamorphosis requires TGFbeta/Activin signaling. Development 138: 269–2703.

Good, R. T., L. Gramzow, P. Battlay, T. Sztal, P. Batterham *et al.*, 2014 The molecular evolution of cytochrome P450 genes within and between *Drosophila* species. Genome Biol. Evol. 6: 1118–1134.

Graveley, B. R., A. N. Brooks, J. W. Carlson, M. O. Duff, J. M. Landolin *et al.*, 2011 The developmental transcriptome of *Drosophila melanogaster*. Nature 471: 473–479.

Grieneisen, M. L., 1994 Recent advances in our knowledge of ecdysteroid biosynthesis in insects and crustaceans. Insect Biochem. Mol. Biol. 24: 115–132.

Guittard, E., C. Blais, A. Maria, J. P. Parvy, S. Pasricha *et al.*, 2011 CYP18A1, a key enzyme of *Drosophila* steroid hormone inactivation, is essential for metamorphosis. Dev. Biol. 349: 35–45.

Haelterman, N. A., L. Jiang, Y. Li, V. Bayat, H. Sandoval *et al.*, 2014 Large-scale identification of chemically induced mutations in *Drosophila melanogaster*. Genome Res. 24: 1707–1718.

He, Q., D. Wen, Q. Jia, C. Cui, J. Wang *et al.*, 2014 Heat Shock Protein 83 (Hsp83) Facilitates Methoprene-tolerant (Met) Nuclear Import to Modulate Juvenile Hormone Signaling. J. Biol. Chem. 289: 27874–27885.

Henrich, V. C., 1995 Comparison of ecdysteroid production in *Drosophila* and *Manduca*: pharmacology and cross-species neural reactivity. Arch. Insect Biochem. Physiol. 30: 239–254.

Hoffmann, J. A., 2003 The immune response of *Drosophila*. Nat. Cell Biol. 426: 33–38.

Huang, D. W., B. T. Sherman, and R. A. Lempicki, 2009 Systematic and integrative analysis of large gene lists using DAVID bioinformatics resources. Nat. Protoc. 4: 44–57.

Huang, X., J. Warren, and L. Gilbert, 2008 New players in the regulation of ecdysone biosynthesis. J. Genet. Genomics 35: 1–10.

Jindra, M., Uhlirova, M., Charles, JP., Smykal, V., Hill, R. J., 2015 Genetic evidence for function of the bHLH-PAS protein Gce/Met as a Juvenile hormone receptor. PLoS Genet. 11: e1005394.

Karim, F., and C. Thummel, 1992 Temporal coordination of regulatory gene-expression by the steroid-hormone ecdysone. EMBO J. 11: 4083–4093.

Kim, S. K., and E. J. Rulifson, 2004 Conserved mechanisms of glucose sensing and regulation by *Drosophila* corpora cardiaca cells. Nature 431: 316–320.

King, R., S. Aggarwal, and D. Bodenste, 1966 Comparative submicroscopic morphology of ring gland of *Drosophila melanogaster* during 2nd and 3rd larval instars. Z. Zellforsch. Mikrosk. Anat. 73: 272.

Koelle, M., W. Talbot, W. A. Segraves, M. T. Bender, P. Cherbas *et al.*, 1991 The *Drosophila ecr* gene encodes an ecdysone receptor, a new member of the steroid-receptor superfamily. Cell 67: 59–77.

Kopp, A., and J. R. True, 2002 Evolution of male sexual characters in the oriental *Drosophila melanogaster* species group. Evol. Dev. 4: 278–291.

Layalle, S., N. Arquier, and P. Léopold, 2008 The TOR pathway couples nutrition and developmental timing in *Drosophila*. Dev. Cell 15: 568–577.

Lemaitre, B., E. Kromer-Metzger, L. Michaut, E. Nicolas, M. Meister *et al.*, 1995 A recessive mutation, immune deficiency (*imd*), defines two distinct control pathways in the *Drosophila* host defense. Proc. Natl. Acad. Sci. USA 92: 9465–9469.

Lemaitre, B., E. Nicolas, L. Michaut, J. M. Reichhart, and J. A. Hoffmann, 1996 The dorsoventral regulatory gene cassette *spatzle/Toll/cactus* controls the potent antifungal response in *Drosophila* adults. Cell 86: 973–983.

Ligoxygakis, P., N. Pelte, C. Y. Ji, V. Leclerc, B. Duvic *et al.*, 2002 A serpin mutant links Toll activation to melanization in the host defence of *Drosophila*. EMBO J. 21: 6330–6337.

Lin, J. I., N. C. Mitchell, M. Kalcina, E. Tchoubrieva, M. J. Stewart *et al.*, 2011 *Drosophila* ribosomal protein mutants control tissue growth non-autonomously via effects on the prothoracic gland and ecdysone. PLoS Genet. 7: e1002408.

Marchal, E., H. Vandersmissen, L. Badisco, S. Van de Velde, H. Verlinden *et al.*, 2010 Control of ecdysteroidogenesis in prothoracic glands of insects: a review. Peptides 31: 506–519.

McBrayer, Z., H. Ono, M. Shimell, J. P. Parvy, R. B. Beckstead *et al.*, 2007 Prothoracicotropic hormone regulates developmental timing and body size in Drosophila. Dev. Cell 13: 857–871.

Minakuchi, C., X. Zhou, and L. M. Riddiford, 2008 *Kruppel homolog 1* (*Kr-h1*) mediates juvenile hormone action during metamorphosis of *Drosophila melanogaster*. Mech. Dev. 125: 91–105.

Mirth, C., J. W. Truman, and L. M. Riddiford, 2005 The role of the prothoracic gland in determining critical weight for metamorphosis in *Drosophila melanogaster*. Curr. Biol. 15: 1796–1807.

Moeller, M. E., E. T. Danielsen, R. Herder, M. B. O'Connor, and K. F. Rewitz, 2013 Dynamic feedback circuits function as a switch for shaping a maturation-inducing steroid pulse in *Drosophila*. Development 140: 4730–4739.

Nagarkar-Jaiswal, S., P.-T. Lee, M. E. Campbell, K. Chen, S. Anguiano-Zarate *et al.*, 2015 A library of MiMICs allows tagging of genes and reversible, spatial and temporal knockdown of proteins in *Drosophila*. eLife 4: 05338.

Niwa, R., and Y. S. Niwa, 2014 Enzymes for ecdysteroid biosynthesis: their biological functions in insects and beyond. Biosci. Biotechnol. Biochem. 78: 1283–1292.

Niwa, R., T. Matsuda, T. Yoshiyama, T. Namiki, K. Mita *et al.*, 2004 CYP306A1, a cytochrome P450 enzyme, is essential for ecdysteroid biosynthesis in the prothoracic glands of *Bombyx* and *Drosophila*. J. Biol. Chem. 279: 35942–35949.

Niwa, R., T. Sakudoh, T. Matsuya, T. Namiki, S. Kasai *et al.*, 2011 Expressions of the cytochrome P450 monooxygenase gene *Cyp4g1* and its homolog in the prothoracic glands of the fruit fly *Drosophila melanogaster* (Diptera: Drosophilidae) and the silkworm *Bombyx mori* (Lepidoptera: Bombycidae). Appl. Entomol. Zool. (Jpn.) 46: 533–543.

Olcott, M. H., M. D. Henkels, K. L. Rosen, F. L. Walker, B. Sneh *et al.*, 2010 Lethality and developmental delay in *Drosophila melanogaster* larvae after ingestion of selected Pseudomonas fluorescens strains. Plos One 5: e12504.

Ono, H., K. F. Rewitz, T. Shinoda, K. Itoyama, A. Petryk *et al.*, 2006 *Spook* and *Spookier* code for stage-specific components of the ecdysone biosynthetic pathway in Diptera. Dev. Biol. 298: 555–570.

Ou, Q., and K. King-Jones, 2013 What goes up must come down: transcription factors have their say in making ecdysone pulses. Curr. Top. Dev. Biol. 103: 35–71.

Ou, Q., A. Magico, and K. King-Jones, 2011 Nuclear receptor DHR4 controls the timing of steroid hormone pulses during *Drosophila* development. PLoS Biol. 9: e1001160.

Ou, Q., J. Zeng, N. Yamanaka, C. Brakken-Thal, M. B. O'Connor *et al.*, 2016 The insect prothoracic gland as a model for steroid hormone biosynthesis and regulation. Cell Rep. 16: 247–262.

Perry, T., J. Q. Chan, P. Batterham, G. B. Watson, C. Geng *et al.*, 2012 Effects of mutations in *Drosophila* nicotinic acetylcholine receptor subunits on sensitivity to insecticides targeting nicotinic acetylcholine receptors. Pestic. Biochem. Physiol. 102: 56–60.

Petersen, T. N., S. Brunak, G. von Heijne, and H. Nielsen, 2011 SignalP 4.0: discriminating signal peptides from transmembrane regions. Nat. Methods 8: 785–786.

Petryk, A., J. Warren, G. Marques, M. Jarcho, L. Gilbert *et al.*, 2003 *Shade* is the *Drosophila* P450 enzyme that mediates the hydroxylation of ecdysone to the steroid insect molting hormone 20-hydroxyecdysone. Proc. Natl. Acad. Sci. USA 100: 13773–13778.

Qiu, Y., C. Tittiger, C. Wicker-Thomas, G. Le Goff, S. Young *et al.*, 2012 An insect-specific P450 oxidative decarbonylase for cuticular hydrocarbon biosynthesis. Proc. Natl. Acad. Sci. USA 109: 14858–14863.

Rewitz, K. F., R. Rybczynski, J. T. Warren, and L. I. Gilbert, 2006 The Halloween genes code for cytochrome P450 enzymes mediating synthesis of the insect moulting hormone. Biochem. Soc. Trans. 34: 1256–1260.

Rewitz, K. F., N. Yamanaka, L. I. Gilbert, and M. B. O'Connor, 2009 The insect neuropeptide PTTH activates receptor tyrosine kinase torso to initiate metamorphosis. Science 326: 1403–1405.

Rewitz, K. F., N. Yamanaka, and M. B. O'Connor, 2013 Developmental checkpoints and feedback circuits time insect maturation. Curr. Top. Dev. Biol. 103: 1–33.

Richard, D. S., and L. I. Gilbert, 1991 Reversible juvenile hormone inhibition of ecdysteroid and juvenile hormone synthesis by the ring gland of *Drosophila melanogaster*. Experientia 47: 1063–1066.

Riddiford, L. M., 1970 Prevention of metamorphosis by exposure of insect eggs to juvenile hormone analogs. Science 167: 287.

Riddiford, L. M., 1993 Hormones and Drosophila development, pp. 899–939 in *The Development of Drosophila*. Cold Spring Harbor Laboratory Press, Cold Spring Harbor, NY.

Rizki, T. M., and R. M. Rizki, 1984   The cellular defense system of Drosophila melanogaster, pp. 579–604 in *Insect Ultrastructure*. Springer, New York.

Rybczynski, R., and L. Gilbert, 2003   Prothoracicotropic hormone stimulated extracellular signal-regulated kinase (ERK) activity: the changing roles of Ca2+- and cAMP-dependent mechanisms in the insect prothoracic glands during metamorphosis. Mol. Cell. Endocrinol. 205: 159–168.

Samakovlis, C., D. A. Kimbrell, P. Kylsten, A. Engstrom, and D. Hultmark, 1990   The immune response in *Drosophila*—pattern of cecropin expression and biological activity. EMBO J. 9: 2969–2976.

Shah, P. K., L. P. Tripathi, L. J. Jensen, M. Gahnim, C. Mason *et al.*, 2008   Enhanced function annotations for *Drosophila* serine proteases: a case study for systematic annotation of multi-member gene families. Gene 407: 199–215.

Shimada-Niwa, Y., and R. Niwa, 2014   Serotonergic neurons respond to nutrients and regulate the timing of steroid hormone biosynthesis in *Drosophila*. Nat. Commun. 5: 5778.

Sliter, T. J., B. J. Sedlak, F. C. Baker, and D. A. Schooley, 1987   Juvenile hormone in *Drosophila melanogaster*. Insect Biochem. 17: 161–165.

Song, Q., X. Sun, and X. Y. Jin, 2003   20E-regulated USP expression and phosphorylation in *Drosophila melanogaster*. Insect Biochem. Mol. Biol. 33: 1211–1218.

St Pierre, S. E., L. Ponting, R. Stefancsik, and P. McQuilton FlyBase Consortium, 2014   FlyBase 102 - advanced approaches to interrogating FlyBase. Nucleic Acids Res. 42: D780–D788.

Tang, H., Z. Kambris, B. Lemaitre, and C. Hashimoto, 2006   Two proteases defining a melanization cascade in the immune system of *Drosophila*. J. Biol. Chem. 281: 28097–28104.

Thummel, C., 2002   Ecdysone-regulated puff genes 2000. Insect Biochem. Mol. Biol. 32: 113–120.

Trapnell, C., A. Roberts, L. Goff, G. Pertea, D. Kim *et al.*, 2012   Differential gene and transcript expression analysis of RNA-seq experiments with TopHat and Cufflinks. Nat. Protoc. 7: 562–578.

Van Hiel, M. B., P. Van Wielendaele, L. Temmerman, S. Van Soest, K. Vuerinckx *et al.*, 2009   Identification and validation of housekeeping genes in brains of the desert locust *Schistocerca gregaria* under different developmental conditions. BMC Mol. Biol. 10: 56.

Vogt, M., 1943   Zur hormonalen Förderung imaginaler Differenzierungsprozesse bei *Drosophila*. Naturwissenschaften 32: 37–39.

Warren, J., A. Petryk, G. Marques, M. Jarcho, J. Parvy *et al.*, 2002   Molecular and biochemical characterization of two P450 enzymes in the ecdysteroidogenic pathway of *Drosophila melanogaster*. Proc. Natl. Acad. Sci. USA 99: 11043–11048.

Warren, J., A. Petryk, G. Marques, J. Parvy, T. Shinoda *et al.*, 2004   *Phantom* encodes the 25-hydroxylase of *Drosophila melanogaster* and *Bombyx mori*: a P450 enzyme critical in ecdysone biosynthesis. Insect Biochem. Mol. Biol. 34: 991–1010.

Wen, D., C. Rivera-Perez, M. Abdou, Q. Jia, Q. He *et al.*, 2015   Methyl farnesoate plays a dual role in regulating *Drosophila* metamorphosis. PLoS Genet. 11: e1005038.

Wigglesworth, V. B., 1954   *The Physiology of Insect Metamorphosis*. Cambridge University Press, Cambridge, UK.

Williams, C. M., 1961   The juvenile hormone. II. Its role in the endocrine control of molting, pupation, and adult development in the *Cecropia* silkworm. Biol. Bull. 121(3): 572–585.

Yamanaka, N., K. F. Rewitz, and M. B. O'Connor, 2013   Ecdysone control of developmental transitions: lessons from *Drosophila* research. Annu. Rev. Entomol. 58: 497–516.

Yamanaka, N., G. Marqués, and M. B. O'Connor, 2015   Vesicle-mediated steroid hormone secretion in *Drosophila melanogaster*. Cell 163: 907–919.

Yeh, S. D., and J. R. True, 2014   The genetic architecture of coordinately evolving male wing pigmentation and courtship behavior in *Drosophila elegans* and *Drosophila gunungcola*. G3 (Bethesda) 4: 2079–2093.

Yoshiyama, T., T. Namiki, K. Mita, H. Kataoka, and R. Niwa, 2006   Neverland is an evolutionarily conserved Rieske-domain protein that is essential for ecdysone synthesis and insect growth. Development 133: 2565–2574.

Communicating editor: J. M. Comeron

Author/s:
Christesen, D; Yang, YT; Somers, J; Robin, C; Sztal, T; Batterham, P; Perry, T

Title:
Transcriptome Analysis of Drosophila melanogaster Third Instar Larval Ring Glands Points to Novel Functions and Uncovers a Cytochrome p450 Required for Development

Date:
2017-02-01

Citation:
Christesen, D; Yang, YT; Somers, J; Robin, C; Sztal, T; Batterham, P; Perry, T, Transcriptome Analysis of Drosophila melanogaster Third Instar Larval Ring Glands Points to Novel Functions and Uncovers a Cytochrome p450 Required for Development, G3-GENES GENOMES GENETICS, 2017, 7 (2), pp. 467 - 479

Persistent Link:
http://hdl.handle.net/11343/221899

File Description:
Published version